PHYSICAL REVIEW A VOLUME 25, NUMBER 2 FEBRUARY 1982

Ingredients of a theory of convective textures close to onset

M. C. Cross
Bell Laboratories, Murray Hill, New Jersey 07974
(Received 20 August 1981)

The patterns of convection to be expected in laterally large Rayleigh-Bénard cells close to onset are analyzed using the amplitude equation approach of Newell and Whitehead and Segel. This equation allows the introduction of a Lyapunov functional, which may be used to order the stability of various patterns. Two competing effects are identified: a surface effect that favors rolls approaching the sidewalls normally, and so tends to produce $O(1)$ rotations of the roll orientation over the cell, and bulk effects that favor straight parallel rolls. The competition between these effects, and the role of defects in the structure, are studied in some simple examples.

I. INTRODUCTION

Theoretical analysis of the effect of the lateral boundaries on the convective pattern in a Rayleigh-Bénard cell has been mostly limited to two simple cases. Firstly, the linearized equations have been studied to determine the onset patterns and their critical Rayleigh numbers. This has been done in cylindrical geometries,[1] for both axially symmetric and nonsymmetric patterns, and for rectangular cells.[2,3] A second class of problems that has been studied is the inclusion of the weak nonlinearities close to onset, but only for certain simple solutions matching the symmetry of the lateral boundaries such as axisymmetric rolls in a cylindrical container[4] or straight rolls parallel to one side of a rectangular container.[5,6] The inclusion of nonlinearity is important, for typically the solutions growing from the more complicated onset patterns become unstable,[5] and the complexity of behavior suggested by the linear analysis[3] may be misleading. In addition there has been numerical work testing the stability of some of the onset patterns in the cylindrical geometry,[7] and for model equations in the rectangular geometry.[8]

On the other hand, a survey of the experimental literature shows the common occurrence of patterns involving large changes in roll orientation over the cell, and often including dislocationlike defects in the rolls (see, for example, Refs. 9—11), although the simple patterns analyzed theoretically have also been observed both in cylindrical[12] and rectangular[13] cells. Two explanations of these complicated patterns seem plausible. It may be that as the Rayleigh number is rapidly increased through the critical value, convection onsets independently in isolated regions with rolls oriented in various directions. As the convection becomes stronger and the different regions come into contact some complicated pattern will form that may persist indefinitely. A second explanation may be that the simple symmetric pattern is in fact unstable towards the more complicated patterns observed. Such an instability has indeed been documented[14] at rather high Rayleigh numbers.

In this paper the influence of lateral boundaries on the convection pattern in the nonlinear regime is studied, without the restriction to simple symmetric patterns of previous work, to investigate the second suggestion. In particular, the effect of lateral boundaries in establishing patterns, in which the direction of the rolls changes slowly but through large angles over the cell, is considered. Borrowing a term from liquid crystal physics, this may be called the study of textures in convection.

The analysis will be performed close to onset in a laterally large system so that use can be made of the "amplitude equation" formalism introduced by Newell and Whitehead[15] and by Segel.[16] This formalism permits the treatment of the spatial inhomogeneities induced by lateral boundaries, together with the weak nonlinearity, in a single equation for the "envelope function" that describes the slow modulation of the basic roll pattern. Also, from the amplitude equation a functional F may be defined[17,18] that decreases in any dynamics of the system (a Lyapunov functional). An ordering of various convection patterns in decreasing values of

this functional may than be used as an ordering of stabilities: on perturbation a pattern may change to one with smaller F, but not to one of higher F. The ordering of stabilities according to the value of F is made rigorous by the presence of small stochastic forcing in the equations, of the form of thermal noise.[17,18] Then any state, even metastable states at local minima of F, will in principle decay to the stable state at the smallest miminum of F. Conventional estimates[17,18] of the magnitude of the stochastic forcing of the amplitude equation due to thermal noise suggest a value too small lead to any probability for the decay of a metastable state over experimental timescales, and in this case higher minima of F may be observed as experimentally stable states. Nevertheless, this ordering of stabilities remains a useful tool in demonstrating the pattern formation tendencies.

The basic approach developed in this paper is to identify two contributions to the functional F: a boundary layer or surface term that favors patterns with rolls approaching the sidewalls normally, implying $O(1)$ rotations in the orientation of the rolls over the cell; and bulk terms that favor straight parallel rolls. It is the competition between these contributions that may lead to interesting textures and textural transitions. The separation into bulk and surface effects is valid in general for

$$\epsilon^{1/2}L >> 1 , \tag{1}$$

where $\epsilon=(R-R_c)/R_c$ with R the Rayleigh number and R_c its critical value in a laterally infinite system, and L is the characteristic lateral size of the system expressed as a ratio to the depth of fluid (i.e., the aspect ratio). The amplitude equation is derived as the lowest nontrivial order in a perturbation expansion in $\epsilon^{1/2}$, and its range of validity is restricted to small ϵ. Equation (1) then implies a laterally large system.

In Sec. II the amplitude equation approach is described, and the existence of a Lyapunov functional governing textural selection is demonstrated. The various contributions to the Lyapunov functional are evaluated in Sec. III. Section IV contains a discussion of the competition between the surface and bulk effects, and considers the relative stability of various possible textures. A full solution to the minimization of the Lyapunov functional requires considerable numerical work, and we restrict ourselves here to a qualitative description of the competition between various types of patterns that might be expected. Finally, conclusions are drawn in Sec. V.

II. AMPLITUDE EQUATION AND LYAPUNOV FUNCTIONAL

Close to the onset of convection, a systematic expansion in the distance above onset ϵ taken to lowest nontrivial order leads to a Lyapunov functional that decreases in any dynamics. In a rectangular geometry with a pattern based on a single set of rolls parallel to the axis and normal to the x direction it is

$$F=\int dx\,dy\left[\tfrac{1}{2}\epsilon^2-\epsilon|A|^2+\tfrac{1}{2}|A|^4+\xi_0^2\left|\left[\partial_x-\frac{i}{2q_0}\partial_y^2\right]A\right|^2\right], \tag{2}$$

where $A(x,y,t)$ is the complex envelope function satisfying the equation[15,16]

$$\tau_0\dot{A}=-\frac{\delta F}{\delta A^*}=(\epsilon-|A|^2)A+\xi_0^2\left[\partial_x-\frac{i}{2q_0}\partial_y^2\right]^2A , \tag{3}$$

and the boundary conditions[19]

$$A(x=\pm L)=0 , \tag{4}$$

$$A(y=\pm M)=A_y(y=\pm M)=0 , \tag{5}$$

for a cell with rigid sidewalls at $x=\pm L$, $y=\pm M$. It is convenient to include the $\frac{1}{2}\epsilon^2$ term in Eq. (2) so that F is zero for a fully saturated, uniform envelope function.

Equation (3) is the amplitude equation introduced by Newell and Whitehead and Segel describing the slow variation on time scale

$$\tau=\epsilon^{-1}t/\tau_0 , \tag{6}$$

and length scales

$$X=\epsilon^{-1/2}x/\xi_0 , \tag{7}$$

$$Y=\epsilon^{-1/4}yq_0{}^{1/2}/\xi_0^{1/2} . \tag{8}$$

of the envelope function $A(x,y,t)$ that describes the modulation of the linear roll pattern. [The reader will often find the amplitude equation written in terms of these scaled variables and a scaled envelope function $\bar{A}=\epsilon^{-1/2}A$ so that all coefficients in the equation are $O(1)$.] The hydrodynamic variables, the horizontal velocity $\vec{u}=(u,v)$, vertical velocity w, and deviation T of the temperature from the linear conducting profile are given by

$$u=\epsilon^{1/2}(Ae^{iq_0x}-\text{c.c.})u_0(z)+O(\epsilon) , \tag{9a}$$

$$v=O(\epsilon)\ , \tag{9b}$$

$$w=\epsilon^{1/2}(Ae^{iq_0x}+\text{c.c.})w_0(z)+O(\epsilon)\ , \tag{9c}$$

$$T=\epsilon^{1/2}(Ae^{iq_0x}+\text{c.c.})T_0(z)+O(\epsilon)\ , \tag{9d}$$

with q_0 the critical wave vector, and u_0, w_0, and T_0, the critical solutions with a normalization factor chosen to make the coefficient of $|A|^4$ in Eq. (2) equal to $\frac{1}{2}$. Equation (3) was originally derived for the mathematically convenient but artificial case of stress-free upper and lower boundaries, but the derivation has since been generalized[20] to the experimentally relevant case of rigid upper and lower boundaries. In fact, recently Siggia and Zippelius[21] have shown that the derivation for *stress-free* boundaries is incorrect except at infinite Prandtl number, and that an additional field (the vertical vorticity) must then be introduced. This difficulty does not arise for rigid boundaries, and we will address our remarks to this case. The parameters τ_0 and ξ_0 are numbers that are $O(1)$ for Prandtl numbers σ of $O(1)$, and are tabulated in Ref. 20.

The boundary conditions Eqs. (4) and (5) were derived by Brown and Stewartson[19] only for stress-free upper and lower boundaries. So far no calculation extending these results to the rigid case has been reported, although Eq. (4) has been confirmed experimentally.[22] In this paper we will assume that Eqs. (4) and (5) remain applicable for the rigid case as well.

Equation (2), the amplitude equation (3) together with the boundary conditions Eqs. (4) and (5) lead to the expression for the time derivative of the functional F:

$$\dot{F}=-2\tau_0\int dx\,dy\,|\dot{A}|^2\ , \tag{10}$$

showing that F decreases in any dynamics and does indeed play the role of a Lyapunov functional.

If the convective rolls are not everywhere nearly parallel, but instead their direction varies slowly but over arbitrarily large angles, more general expressions than Eqs. (2) and (3) are needed. An expression for F involving only the slow variables defined by Eqs. (6)–(8) has not been derived for this case. Instead a real order parameter $\psi(r,t)$ is defined[18,20,23] that includes the rapid sinusoidal variation of the rolls, so that the hydrodynamic variables are given by

$$\vec{u}(\vec{r},z,t)=\vec{\nabla}\psi(\vec{r}t)(iq_0)^{-1}u_0(z)+O(\epsilon)\ , \tag{11a}$$

$$w(\vec{r},z,t)=\psi(\vec{r},t)w_0(z)+O(\epsilon)\ , \tag{11b}$$

$$T(\vec{r},z,t)=\psi(\vec{r},t)T_0(z)+O(\epsilon)\ , \tag{11c}$$

with $\vec{r}$ the horizontal coordinate and $\vec{\nabla}$ the corresponding gradient. The order parameter may be shown to satisfy

$$\tau_0\dot{\psi}=-\frac{\delta F}{\delta\psi}\ , \tag{12}$$

where

$$F=\int d^2r\{\tfrac{1}{2}\epsilon^2-\tfrac{1}{2}\epsilon\psi^2+\tfrac{1}{4}\bar{g}\psi^4+\tfrac{1}{2}(\xi_0^2/4q_0^2)[(\nabla^2+q_0^2)\psi]^2\}\ . \tag{13}$$

The quartic term in Eq. (13) is written for the case of a single set of rolls locally, present, and then $\bar{g}=\frac{1}{3}$. To treat the case of superimposed rolls $\bar{g}$ must be replaced by a nonlocal but short-ranged kernel. Also the gradient term should strictly be the Fourier transform of $(q-q_0)^2|\psi_q|^2$, with ψ_q the Fourier transform of $\psi(\vec{r})$. The expression used in Eq. (13) reduces to this form to the lowest order in ϵ that we are considering, but includes higher-order corrections that will be incorrect.

Equations (12) and (13) reduce[23] to the amplitude equation on the substitution

$$\psi(\vec{r},t)=[A(x,y,t)e^{iq_0x}+\text{c.c.}]\ , \tag{14}$$

with A assumed varying on the slow scales Eq. (9), on coarse graining over a few wavelengths $2\pi q_0^{-1}$, and if only the lowest-order terms in ϵ are retained. The boundary conditions Eqs. (4) and (5) are reproduced by requiring at the boundaries

$$\psi=\hat{s}\cdot\vec{\nabla}\psi=0\ , \tag{15}$$

with $\hat{s}$ the surface normal. These conditions also reproduce to lowest order the boundary conditions recently derived[24] for rolls approaching the sidewall at an arbitrary angle, although higher-order effects (such as the amplitude of the conjugate rolls discussed there) will again be incorrect in numerical details.

With the more general definition F retains the property of a Lyapunov functional

$$\dot{F}=-\tau_0\int d^2r(\dot{\psi})^2\ , \tag{16}$$

and Eqs. (12), (13), and (15) are the generalizations required to allow the study of convective textures. They are correct only to the order in ϵ of the original amplitude equation, and the terms higher-order in ϵ implied by the expressions will be in error. Since, however, at these higher orders in ϵ no

Lyapunov functional is likely to exist, such corrections are in any case of no use in the present work. Note that once F is proven to be a Lyapunov functional for the more general situation, we are free to use either expression, with Eq. (2) a local contribution to the total F from a region where the x direction is chosen locally as normal to the rolls.

III. TEXTURAL CONTRIBUTIONS TO F_L

Two competing contributions to F may be identified: a boundary layer or surface contribution, and bulk contributions. Close to the sidewalls the convection is suppressed, and the envelope function goes to zero. It heals to its bulk value in a distance typically $O(\epsilon^{-1/2}\xi_0)$, but depending on the orientation of the rolls. This leads to a boundary layer contribution to F of order $\epsilon^{3/2}$ per unit length, which depends on the orientation at which the rolls approach the surface. On the other hand, well away from the sidewalls the magnitude of the envelope function should mostly take on the maximum value consistent with the slow variation of the roll orientation. There will then be a bulk contribution to F depending on this slow variation. In addition, it turns out that to allow a particular kind of bending of the roll structure localized defects must be allowed in the roll pattern, corresponding to the ending of a pair of rolls (dislocations). Around the dislocation point the magnitude of convection will be supressed according to Eqs. (3) or (12) over a core region of size $O(1)$ in the slow variables X, Y. This leads to an additional cost to F. Finally we consider the possibility of a grain boundary or "internal surface" line between regions of rolls with differing orientations, allowing abrupt (i.e., over the length scale $\epsilon^{-1/2}\xi_0$) jumps in the roll orientation in the bulk of the cell.

In the analysis of these effects the separation of length scales $\epsilon^{1/2}L >> 1$ will be repeatedly used. This implies that the healing of the magnitude of the convection $|A|$, near a sidewall or the core of a defect, takes place on a length scale ($\lesssim \epsilon^{-1/2}$) much shorter than the size of the system L that governs the length scale over which the orientation of the rolls must change. Thus, for example, to investigate the surface contribution we may usually simplify the calculation by considering straight rolls approaching a straight boundary.

A. Surface contribution

The approach of the envelope function to zero at a rigid sidewall for rolls parallel or perpendicular to a plane sidewall was investigated by Brown and Stewartson.[19] The question of rolls approaching at an arbitrary angle was studied only recently.[24] There it was shown that rolls may indeed approach at an arbitrary angle, and that the healing of the envelope function is then described by

$$\xi_0^2\cos^2\theta\frac{d^2A}{dx^2}+\epsilon A-|A|^2A=0\,,\qquad A(x=0)=0\,, \tag{17}$$

with x measuring the distance from the sidewall and θ the angle between the roll normal $\hat{n}$ and the surface normal $\hat{s}$. These equations are also implied by Eqs. (12) and (15). [In fact, in either case to satisfy the boundary conditions, small amplitude "conjugate rolls" at an angle $-\theta$ are excited in the boundary layer,[24] but these do not affect Eq. (17) or the contribution to F to the order needed.]

The solution to Eqs. (17) is

$$A=\epsilon^{1/2}\tanh(x/\sqrt{2\xi})\,, \tag{18}$$

with $\xi=\epsilon^{-1/2}\xi_0\cos\theta$, leading to a boundary layer contribution to the Lyapunov functional per length

$$F_s=\epsilon^{3/2}f_s(\hat{n}\cdot\hat{s})\,, \tag{19}$$

with

$$f_s=\tfrac{2}{3}\sqrt{2}\xi_0\,, \tag{20}$$

The boundary layer contribution is minimized for $\hat{n}\cdot\hat{s}=0$, which corresponds to rolls approaching normal to the boundary. In this limit (in fact $\theta'=\pi/2-\theta\lesssim\epsilon^{1/4}$) Eq. (19) is not valid, since the fourth-order gradient terms omitted in Eq. (17) then become important. Their inclusion leads to the result for $\theta'\to 0$

$$F_s\sim\epsilon^{7/4}[1+O(\epsilon^{-1/4}\theta')]\,, \tag{21}$$

which is usually negligible compared with terms such as Eq. (19) in the limit of validity of the approach, $\epsilon << 1$. The tendency of rolls to come in normal to the surface was previously observed by Davis[2] from a linear calculation (see also Segel[16]) and our work extends this conclusion into the nonlinear regime. Pomeau and Zaleski[25] have shown in fact that for rolls parallel to a plane boundary, there is a *linear* instability towards nucleation of a set of normal rolls in the boundary layer, and their result should also apply for rolls approaching at an arbitrary angle, not normal. In a finite system the second set of rolls may be suppressed by other sidewalls or by the curvature of the surface. For example, the instability for concentric rolls parallel

to a cylindrical surface towards radial rolls in the boundary layer may be shown to be suppressed for curvatures $r^{-1} \gtrsim \epsilon$, although an instability to straight rolls may still exist (Sec. IV).

B. Bulk contributions

Away from the sidewalls we expect the magnitude of the envelope function to reach the saturation value consistent with the slow variation of the roll direction. It is convenient to introduce variables $\hat{n}$, a unit vector normal to the rolls, and δq, the deviation of the local roll wave vector from q_0. Ignoring gradients of the magnitude of the envelope function, which will lead to small correction terms, and then minimizing the expression for F locally with respect to the magnitude of the envelope function leads to an expression for the bulk contribution:

$$F_B = \epsilon \int d^2r [\tfrac{1}{4}(\mathrm{div}\hat{n})^2 + (\delta q)^2] \ . \tag{22}$$

This expression can be derived from Eq. (13) by writing

$$\psi = |A| e^{i\zeta} + \text{c.c.} \ , \tag{23}$$

with

$$\vec{\nabla}\zeta = (q_0 + \delta q)\hat{n} \ , \tag{24}$$

or by taking Eq. (2) with locally $A = |A| e^{i\phi}$ and

$$\hat{n} \approx (1, q_0^{-1}\partial_y \phi) \ , \tag{25}$$

$$\delta q \approx \partial_x \phi + \tfrac{1}{2} q_0^{-1} (\partial_y \phi)^2 \ . \tag{26}$$

In addition these identities imply the constraint

$$\mathrm{curl}_z \hat{n} = q_0^{-1} (\hat{n} \times \vec{\nabla} \delta q)_z \ , \tag{27}$$

so that a texture of $\hat{n}$ with nonzero $\mathrm{curl}_z \hat{n}$ (i.e., with "bend" in the language of liquid crystal physics) implies a deviation of the roll wave vector from q_0. Now for the convecting state to be stable with respect to the conducting state we expect over most of the cell,

$$\delta q \lesssim \epsilon^{1/2} \ . \tag{28}$$

Such an nonzero δq is, according to Eq. (27), typically sufficient to allow nonzero $\mathrm{curl}_z \hat{n}$ corresponding to no more than $O(\epsilon^{1/2})$ variations of $\hat{n}$ over the cell. Therefore, in the discussion of convective textures where we are interested in $O(1)$ variations of $\hat{n}$, as a first approximation we may take $\delta q = 0$ over the bulk of the cell, leading to

$$F_B \simeq \epsilon \int d^2r \tfrac{1}{4} (\mathrm{div}\hat{n})^2 \ , \tag{29}$$

together with the constraint

$$\mathrm{curl}_z \hat{n} = 0 \ . \tag{30}$$

Relaxing the restriction $\delta q = 0$ will lead to small corrections in $\hat{n}$ and F.

C. Defect contribution

It will be seen in Sec. IV A that Eq. (27) or Eq. (30) provides a strong restriction on the possible textures. The origin of these constraints is the single value assumed by the phase of the order parameter ζ [Eq. (24)]. They may therefore be relaxed if there exists points where $|A| \to 0$ so that the phase becomes undefined. Such isolated points are dislocations in the rolls, shown schematically in Fig. 1(a). It is easy to see that dislocations permit textures with bending of $\hat{n}$ [see Fig. 1(b)]. A careful calculation of the additional F implied by such a texture requires knowledge of the defect distribution. However, in a large system it is useful to consider a coarse grained description averaging over an area a enclosed by a contour C containing several defects. Then, defining a coarse grained bending by

$$\langle \mathrm{curl}_z \hat{n} \rangle = \frac{1}{a} \int_c \hat{n} \cdot d\vec{l} \ , \tag{31}$$

leads to the result

$$\langle \mathrm{curl}_z \hat{n} \rangle = 2\pi q_0^{-1} \rho_D(r) \ , \tag{32}$$

with $\rho_D(r)$ the dislocation density. The contribution to F per unit area from isolated defects may then be written

$$F_D = (q_0/2\pi) \langle \mathrm{curl}_z \hat{n} \rangle F_c \ , \tag{33}$$

where F_c is the core contribution of a single defect,

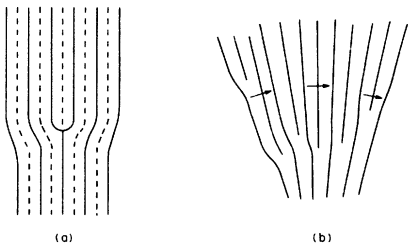

FIG. 1. Dislocations in the roll structure. (a) Schematic drawing of a single dislocation point in the rolls. (b) The presence of dislocations allows a fanlike pattern of rolls. The arrows indicate the direction of the normal to the rolls $\hat{n}$, which is "bending" in the liquid crystal language.

and interactions between the dislocations have been ignored since they generally decay exponentially with separation.[26] The core contribution F_c arises from the depressed magnitude of the envelope function approaching the singular point. It is estimated to be (Appendix A)

$$F_c = \gamma \epsilon^{5/4} , \tag{34}$$

where γ is an $O(1)$ number that requires numerical evaluation.

The expression for the defect contribution F_D in Eq. (33) has assumed defect separations [typically $O(L^{-1})$ if the defects are distributed over most of the cell] large compared with the core radius $O(\epsilon^{-1/2})$. This is justified by the basic assumption Eq. (1). However, if the dislocations are instead arranged along a single line, the separation implied by Eq. (32) becomes $O(1)$. Such an arrangement (Fig. 2) may be called a grain boundary.[27] A small-angle grain boundary may indeed be treated as a line of well-separated dislocations. For larger angles where the cores would overlap it is better treated as an "internal surface" between regions decribed by different envelope functions. Such a calculation is described in Appendix B. This leads to the contribution per length of grain boundary

$$F_G = \epsilon^{3/2} \cos\theta \xi_0 f_G[\beta(\theta)] , \tag{35}$$

where $\beta(\theta)$ is a parameter depending on Prandtl number describing the interaction of two sets of rolls at an angle 2θ. The function f_G has bounds

$$f_G(z) \leq z^{1/2} \tag{36a}$$

and

$$f_G(z) \leq 4\sqrt{2}/3 , \tag{36b}$$

where the bounds become good estimates for z small (36a) and z large (36b), respectively. The values of f_G are graphed in Fig. 3 for various Prandtl numbers. For very small θ ($\theta \lesssim \epsilon^{1/4}$) a description in terms of isolated dislocations (of order $q_0\theta$ per length of grain boundary) is better and leads to a lower value:

$$F_G \sim \epsilon^{5/4}\theta, \quad \theta \lesssim \epsilon^{1/4} . \tag{37}$$

D. Summary

Three contributions to the Lyapunov functional F have been identified: a surface contribution, a bulk contribution, and a defect contribution. The surface contribution tends to produce $O(1)$ rotations of the roll structure over the cell, whereas the bulk and defect contributions are reduced by a texture of straight parallel rolls. To compare their magnitudes the spatial gradients of the roll orientation are taken to be $O(L^{-1})$ with L the characteristic aspect ratio of the cell. This gives the results displayed in Table I. Note that the analysis has assumed $\epsilon << 1$, so that the amplitude equation approach is valid and F is a useful quantity, but $\epsilon^{1/2}L >> 1$, so that surface and bulk contributions may be conveniently separated. In addition, textures consisting locally of a single set of rolls have been assumed. Superimposed rolls (e.g., locally squares or hexagons) lead to a much larger bulk contribution[28] $O(\epsilon^2 L^2)$ and may be safely ignored over the bulk of the cell.

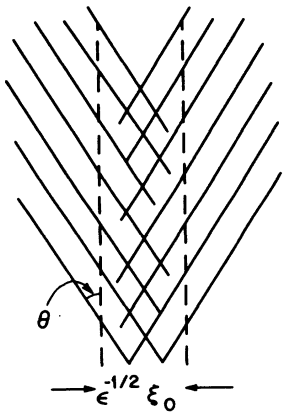

FIG. 2. A large-angle grain boundary. In the boundary thickness of order $\epsilon^{-1/2}\xi_0$ the pattern consists of a superposition of the two roll patterns.

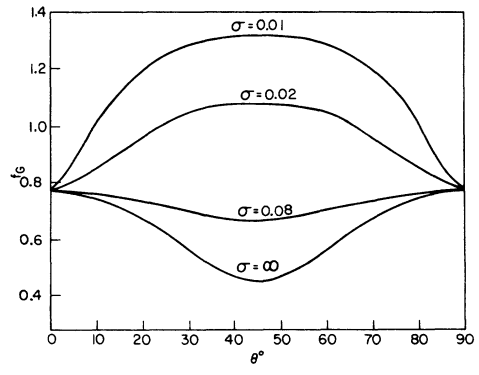

FIG. 3. The parameter f_G giving the grain boundary cost to the Lyapunov functional per length of boundary as a function of the angle θ of Fig. 2.

TABLE I. Contributions to the Lyapunov functional F. Taking spatial gradients of the roll orientation to be $O(L^{-1})$ the orders of magnitudes of the various contributions to F are compared.

	Contribution to F	Contribution to F/ϵ
Surface $\langle \hat{n}\cdot\hat{s} \rangle$	$\epsilon^{3/2}L$	$\epsilon^{1/2}L$
Bulk textural $\langle (\mathrm{div}\hat{n})^2 \rangle$	ϵ	1
Dislocation $\langle \mathrm{curl}_z \hat{n} \rangle$	$\epsilon^{5/4}L$	$\epsilon^{1/4}L$
Roll superposition	$\epsilon^2 L^2$	$(\epsilon^{1/2}L)^2$

IV. ANALYSIS OF TEXTURES

We look for the "most stable" pattern of rolls as the one giving the lowest mimimum of F, which is the sum of contributions displayed in Table I. A complete solution to this problem requires numerical solution of the order parameter Eq. (13). Here we will compare the values of F for some simple configurations in various geometries to demonstrate the types of effects that must come into the complete solution. In particular, we will emphasize the scaling of various terms with ϵ and L, so that the limit $\epsilon \to 0$, $\epsilon^{1/2}L >> 1$ may be easily studied. We first look at possible textures in the absence of defects in the bulk of the cell and then consider modifications on relaxing this constraint.

A. Defect-free textures

In the absence of dislocations the constraint Eq. (30) leads to the condition that contours of constant $\hat{n}$ lie *along* $\hat{n}$. This implies that if the orientation of a particular roll is known everywhere, then the orientation of the other rolls is fixed by this construction. The boundary layer contribution F_s may lead to a global selection of a particular pattern satisfying this constraint, but in general local adjustments to reduce F_s will not be possible. Furthermore, for a curved roll the construction implies orientational singularities at distances of order of the radius of curvature, which for the large curvatures required to minimize F_s everywhere, will usually be within the cell. In this case, if only point orientational singularities are permitted, the rolls must form segments of concentric circles. (The possibility of line orientational singularities will be considered later.) Thus, we are led to look at the competition between bulk and surface contributions for textures of concentric circles, although other textures are certainly possible.

1. *Rectangular cell $L \times M$*

First consider a long, thin cell $L >> M$. In this case, for textures of straight parallel rolls F_s is clearly minimized by rolls parallel to the short side of the cell, Fig. 4(a). This is the extension of the well-known result of Davis[2] into the fully nonlinear regime $\epsilon^{1/2}L >> 1$. Such a pattern is often observed close to onset, e.g., Ref. 13. For widths $M \lesssim \epsilon^{-1/2}$ this is probably the most stable pattern. For larger widths the boundary layer instability discussed in Sec. III A will arise. The details of the behavior near the endwalls is then complicated, but if defects are excluded the final state may be as in Fig. 4(a), but with small amplitude cross rolls in the boundary layers at the endwalls.

For L and M of comparable size it is easy to devise textures that reduce F_s from the value for straight rolls. For example, for the case $L = M$ the texture of Fig. 4(b), consisting of circles centered on one corner, reduces F_s by a factor of 0.88 from the value of straight rolls parallel to one side. The bulk textural contribution for Fig. 4(b) is larger than that for straight rolls, but is negligible for $\epsilon^{1/2}L >> 1$. Again the effect of the surface instability on these two textures is not clear.

2. *Circular-cylindrical cell, radius L*

An interesting comparison in this case is given by textures of concentric rolls [Fig. 5(a)] or of straight rolls [Fig. 5(b)]. The pattern of concentric rolls was observed by Koschmieder and Pallas,[7] whereas a pattern similar to Fig. 5(b) may have been observed as a stationary stable state by Chen and Whitehead[29] and in small cells by Stork and Muller.[30] It is easy to see that for $\epsilon^{1/2}L >> 1$, the texture of straight rolls is the more stable since it

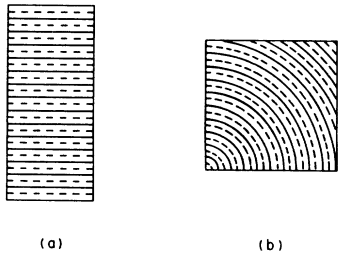

FIG. 4. Schematic drawing of suggested roll patterns in (a) a long thin rectangle and (b) a square cross section.

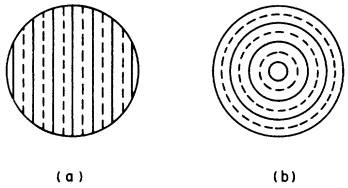

FIG. 5. Schematic drawing of suggested roll patterns in a circular cross section.

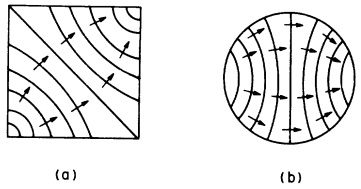

FIG. 6. Textures with defects. The lines are to be thought of as locally along the roll directions, and not as actual fluid contours. The arrows indicate the direction of $\hat{n}$. These textures imply the presence of dislocations distributed over the cell.

leads to a lower F_s (by the factor $2/\pi$). The bulk textural contribution also favors this result, but is again negligible. The result that straight rolls should be more stable than concentric rolls in a large cylindrical geometry was suggested before[23] by an approximate analysis for $\epsilon^{1/2}L=O(1)$. A similar conclusion was reached by Charlson and Sani[7] for some much smaller cells.

B. Textures with isolated dislocations

The examples considered in Sec. IV A demonstrate the tendency of the rolls to come in everywhere perpendicular to the sidewall. For a closed contour boundary, this is inconsistent with the constraint implied by the absence of defects. Relaxing this constraint leads to a certain number of dislocations, with the corresponding cost in F. This must be compared with the gain in the surface contribution.

The number of dislocations N_D is easily calculated using

$$N_D=(q_0/2\pi)\int d^2r\,|\,\mathrm{curl}_z\hat{n}\,| =(q_0/2\pi)\left|\left[\int_+-\int_-\right]\hat{n}\cdot d\vec{l}\,\right|, \tag{38}$$

where the cell is divided into regions $\pm$ of positive and negative $\mathrm{curl}_z\hat{n}$. For isolated dislocations the contribution to F is then N_DF_c with F_c given by Eq. (34).

As examples, consider the textures in Fig. 6, which may be thought of as Figs. 4(b) and 5(b) distorted so that the rolls come in perpendicular to the sidewalls. The numbers of dislocations, given by the integral in Eq. (38) are

$$N_D(\text{square})=(4-2\sqrt{2})q_0L/2\pi\,, \tag{39a}$$

$$N_D(\text{cylinder})=2(\pi-2)q_0L/2\pi\,, \tag{39b}$$

with the corresponding dislocation cost F_D of N_DF_c. On the other hand, the change in the surface contributions [from those of Figs. 4(b), and 5(b)] are

$$\delta F_s(\text{square})\simeq-0.88\times4Lf_s\,, \tag{40a}$$

$$\delta F_s(\text{cylinder})\simeq-4Lf_s\,, \tag{40b}$$

with f_s given by Eq. (20). Notice that both F_D and δF_s are proportionality to L, the characteristic size of the system. The constants of proportionality are, however, $O(\epsilon^{5/4})$ and $O(\epsilon^{3/2})$, respectively, so that in the formal limit $\epsilon\to0$ the dislocation cost always outweighs the surface gain, and the simpler dislocation free textures are more stable. Simple power-counting arguments suggest this result is true in general.

This conclusion may change, however, if ϵ is retained small, but the limit $\epsilon\to0$ is not taken. An example demonstrating this is convection in an annual region between r and $r+\delta r$ with $\epsilon^{1/2}\delta r$, $\epsilon^{1/2}r>>1$ but $\delta r/r<<1$. We now compare the texture of radial rolls Fig. 7(a), which are normal to both sidewalls but contain dislocations, to that of straight rolls Fig. 7(b). Since the number of defect is now

$$N_D=(q_0/2\pi)\int\hat{n}\cdot d\vec{l}=q_0\delta r\,, \tag{41}$$

giving a defect contribution $F_D\sim\epsilon^{5/4}\delta r$, whereas the difference in the surface contribution is propor-

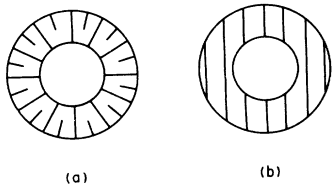

FIG. 7. Schematic drawing of possible textures in an annular cross section.

tional to $\epsilon^{3/2}r$, we find that the texture with dislocations Fig. 7(a) is the more stable for

$$\epsilon^{1/4} \gtrsim \left\lceil \frac{\delta r}{r} \right\rceil . \tag{42}$$

This result suggests a transition for $\epsilon \sim (\delta r/r)^4$, which may be made arbitrarily small. Although the geometry is certainly a special case, chosen to emphasize surface effects, it provides an interesting example where the tendency of rolls to come in normal to the boundary may favor a texture involving roll dislocations.

C. Textures with grain boundaries

In Sec. IV B the defects were assumed to be isolated dislocations. It is also of interest to consider textures involving large-angle grain boundaries. The question arises whether, to satisfy the tendency of rolls to come in normal to the sidewalls, it is favorable to introduce a large-angle grain boundary. Since both contributions to F scale as $\epsilon^{3/2}L$, analyzing the competition involves a comparison of the numerical prefactors in Eqs. (35) and (19).

As an example, consider the possibility of a grain boundary along the diagonal of a square cell, Fig. 8, compared with the texture of circular rolls, Fig. 4(b). The grain boundary contribution in Fig. 8 is

$$F_G \approx \sqrt{2}\epsilon^{3/2}L\xi_0\overline{f_G \cos\theta} , \tag{43}$$

where the bar averaging over the angle θ of the grain boundary along its length. Compare this with the change in F_S from the texture in Fig. 4(b):

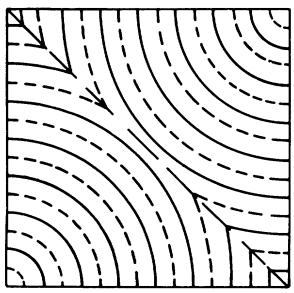

FIG. 8. A texture in a square cross section with a large-angle grain boundary (of varying θ) along a diagonal.

$$\delta F_s = -0.88(4\sqrt{2}/3)\epsilon^{3/2}L\xi_0$$
$$= -1.66\epsilon^{3/2}L\xi_0 . \tag{44}$$

Using the values for f_G from Fig. 3, suggests for not too small Prandtl numbers

$$F_G + \delta F_S < 0 , \tag{45}$$

so that the texture with a grain boundary is then more stable.

V. Conclusions

Various ingredients that tend to favor particular textures close to onset (in the sense of reducing the Lyapunov functional F) have been identified. We find a strong tendency for the rolls to come in normally to a rigid sidewall, in this way minimizing the thickness of the boundary layer over which convection is suppressed. However, close to onset the roll wavelength is rather precisely fixed, so that a condition of rolls normal to all sidewalls implies the presence of defects in the cell. The analysis suggests that in the limit $\epsilon \to 0$ but $\epsilon^{1/2}L >> 1$, the cost to F of isolated dislocations outweighs the reduced surface contribution, and such textures will not be the most stable. Geometries may be devised that probably do have most stable textures with isolated defects at small but finite ϵ. In addition, at least at not too small Prandtl numbers, textures with grain boundary defects may become favorable.

We have assumed an ordering of stabilities according to decreasing values of the functional F. In practice, in the absence of significant stochastic forcing, any local minimum may be observed as steady state over long times. In this case the results may be useful in understanding relaxation towards these minima.

The analysis has been done only for small ϵ, a region where two dynamic length scales exist (in addition to the cell size L): the roll wavelength $2\pi q_0^{-1}$ and the magnitude healing length $O(\epsilon^{-1/2}q_0^{-1})$. It is unclear how many of the qualitative effects derived is this limit may extend to larger Rayleigh numbers, where only a single-length scale governs the dynamics. One possible difference is that at larger Rayleigh numbers the roll wavelength may suffer larger distortions, allowing more roll bending without necessitating dislocations. Few systematic experiments have been done to study the textures close to onset in large cells where our analysis should be valid. Krishnamurti[9] has reported results for rectangular,

cylindrical, and annular containers for R/R_c of 1.1 or 1.2 using a high Prandtl number oil. She remarks on the tendency of rolls to come in normal to the sidewall in each case. The texture observed in the rectangular cell consists of rolls parallel to the short side, with some cross-roll modulations of the two rolls nearest each end, as would be expected from the discussion of Sec. III A. Bergé[13] shows similar results. Both circular and annular cells Krishnamurti finds lead to defected textures, although the reproducibility of the details of the textures is not remarked upon. On the other hand, at slightly higher Rayleigh numbers the textures observed by Chen and Whitehead[29] in the circular container seem better described as straight rolls with some cross roll modulation near the sidewalls, although this result may be biased by the initial pattern of straight rolls used. In an annular container they observe a texture reminiscent of Fig. 7(a). At higher Rayleigh numbers the presence of isolated dislocations seems to be a more general feature than suggested by our small ϵ analysis (e.g., Refs. 10 and 11). Whether this difference arises from the defects being frozen in from some initial condition, or simply reflects the difference of a larger Rayleigh number or rather small cell sizes, is not known.

Even our analysis at small ϵ has been descriptive rather than quantitative. It would be interesting to study the trends suggested by this approach further by numerical solution of the amplitude equations [for example, Eqs. (12) and (13)]. A first step has recently been reported by Manneville.[31] Further studies including, for example, a study of the dependence on initial conditions would provide useful information for comparison with experiment.

Finally it should be remarked that the amplitude equation is derived as a truncation of an expansion in $\epsilon^{1/2}$. A solution minimizing the functional F is a static solution at the order of the expansion giving the amplitude equation, but may not be static when higher-order effects are included. In particular, time variations on the scale set by Eq. (6) are ruled out, but variation on a slower time scale may occur. Even the pattern labeled "most stable" is conceivably not stationary on these longer timescales.

ACKNOWLEDGMENTS

The author thanks Daniel S. Fisher, Eric Siggia, and Annette Zipelius for useful conversations on various aspects of this work.

APPENDIX A: DISLOCATION CORE CONTRIBUTION TO F_L

Assume a roll pattern with straight rolls to the y axis except for distortions induced by adding an extra roll pair at $x=0$, $y\geq 0$. If the deviations of the roll normal from the x axis are small over the regions contributing to F, we may use the expression Eq. (2). The core contribution will be of order

$$F_c \sim \epsilon^2 \text{core area} , \tag{A1}$$

where the core is the size of the region where the magnitude $|A|$ is depressed.

The dependence $F_c(\epsilon)$ may be readily found by transforming to the scaled variables X, Y according to Eqs. (7) and (8) together with

$$\bar{A}=\epsilon^{-1/2}A , \tag{A2}$$

$$\bar{F}=\epsilon^{-5/4}(q_0/\xi_0^3)^{1/2}F , \tag{A3}$$

so that

$$\bar{F}=\int dX\,dY\left[\tfrac{1}{2}-|\bar{A}|^2+\tfrac{1}{2}|\bar{A}|^4+\left|\left[\partial_X-\frac{i}{2}\partial_Y^2\right]\bar{A}\right|^2\right] , \tag{A4}$$

with the stationary dislocation solutions determined by

$$\frac{\delta\bar{F}}{\delta\bar{A}^*}=0=\bar{A}-|\bar{A}|^2\bar{A}+\left[\partial_X-\frac{i}{2}\partial_Y^2\right]^2\bar{A} , \tag{A5}$$

together with the condition

$$\int_c \bar{\nabla}\phi\cdot d\vec{l}=2\pi , \tag{A6}$$

where the contour C surrounds the dislocation point. Equation (A5) will lead to a magnitude $|\bar{A}|$ that heals to unity in distances $O(1)$ in the scaled variable. These equations have been studied by Toner and Nelson,[26] who show that the integral Eq. (A4) converges at long distances so that

$$\bar{F}_c=O(1) , \tag{A7}$$

where the value of the constant must be evaluated by numerical solution. Returning to the unscaled variables according to Eq. (A3) gives the core contribution to F:

$$F_c=\alpha\epsilon^{5/4} , \tag{A8}$$

where all constants are absorbed into the $O(1)$ number α.

APPENDIX B: GRAIN BOUNDARY CONTRIBUTION TO F_L

A large-angle grain boundary may be treated as an "internal surface" separating regions described by different envelope functions A_1 and A_2. If x is the coordinate normal to the grain boundary (imagining the geometry of Fig. 2) then the contribution to F per length of grain boundary is $\epsilon^{3/2}\xi_0\cos\theta f_G$ where, assuming $\bar{A}_1$, $\bar{A}_2$ both real

$$f_G=\int dX\{\tfrac{1}{2}-(\bar{A}_1^2+\bar{A}_2^2)+\tfrac{1}{2}[\bar{A}_1^4+2(\beta+1)\bar{A}_1^2\bar{A}_2^2+\bar{A}_2^4]+(\partial_X\bar{A}_1)^2+(\partial_X\bar{A}_2)^2\} \tag{B1}$$

where here X is the scaled normal coordinate

$$X=\epsilon^{-1/2}/\xi_0\cos\theta\ , \tag{B2}$$

and for angles θ not too close to $\frac{1}{2}\pi$ the fourth-order gradient terms may be neglected. The parameter $\beta(\theta)$ was introduced by Newell and Whitehead[15] to describe the superposition of roll structures, and is discussed further in Ref. 23. Its value for the useful case of rigid top and bottom boundaries may be calculated from Ref. 20.

We seek a minimum of f_G where $\bar{A}_1(-\infty)=1$, $\bar{A}_1(+\infty)=0$, and $\bar{A}_2(-\infty)=0$, $\bar{A}_2(+\infty)=1$. It is then convenient to introduce variables η, χ defined by

$$\bar{A}_1=\eta\cos\chi\ , \tag{B3}$$

$$\bar{A}_2=\eta\sin\chi\ , \tag{B4}$$

so that $\eta(\pm\infty)=1$, $\chi(-\infty)=0$ and $\chi(+\infty)=\pi/2$ and

$$f_G=\int dX[\tfrac{1}{2}(1-\eta^2)^2+(\partial_X\eta)^2+\tfrac{1}{4}\beta\eta^4\sin^2\chi+(\eta\partial_X\chi)^2]\ . \tag{B5}$$

The minimum of f_G must be found numerically. We may place upper bounds using some simple variational ansatz. For $\beta=0$ it is clear that the solution will have $\eta=1$ everywhere, with χ varying arbitrarily slowly, leading to $f_G=0$. For small β a good trial solution is to assume $\eta=1$, with variation only in χ:

$$f_G\le\int dX[\tfrac{1}{4}\beta\sin^2\chi+(\partial_X\chi)^2]\ . \tag{B6}$$

This may be readily minimized to give

$$f_G\le[\beta(\theta)]^{1/2} \tag{B7}$$

with the bound becoming a good estimate for β small. On the other hand, for large β only when η is small will χ change significantly. In this limit an ansatz of η going linearly to zero either side of $x=0$ should be good giving [cf. Eq. (20)]

$$f_G\le 4\sqrt{2}/3\ , \tag{B8}$$

where the bound becomes a good estimate for large β. Values of f_G calculated numerically for various Prandtl numbers are displayed in Fig. 3.

For θ close to $O(\theta\lesssim\epsilon^{1/4})$ the grain boundary will appear as a line of isolated dislocations, and the results of Appendix A should be used.

[1]G. S. Charlson and R. L. Sani, Int. J. Heat Mass Transfer 13, 1479 (1970).
[2]S. H. Davis, J. Fluid Mech. 30, 465 (1976).
[3]C. Normand, Z. Angew. Math. Phys. 32, 81 (1981).
[4]S. N. Brown and K. Stewartson, Proc. R. Soc. London Ser. A 360, 455 (1978).
[5]P. G. Daniels, Proc. R. Soc. London Ser. A 358, 173 (1977); Mathematica 25, 216 (1978).
[6]M. C. Cross, P. G. Daniels, P. C. Hohenberg, and E. D. Siggia, Phys. Rev. Lett. 45, 898 (1980).
[7]G. S. Charlson and R. L. Sani, J. Fluid Mech. 71, 209 (1975).
[8]Y. Pomeau and P. Manneville, Phys. Lett. 75A, 296 (1980); Y. Pomeau and S. Zaleski, J. Phys. (Paris) 42, 515 (1981).
[9]R. Krishnamurti, J. Fluid Mech. 60, 285 (1973).
[10]G. E. Willis, J. W. Deardorff, and R. C. J. Somerville, J. Fluid Mech. 54, 351 (1972).
[11]J. Gollub and J. F. Steinman, Phys. Rev. Lett. 47, 505 (1981).
[12]E. L. Koschmieder and S. G. Pallas, Int. J. Heat Mass Transfer 17, 991 (1974).
[13]P. Berge, in *Fluctuations, Instabilities and Phase Transitions,* edited by T. Riste (Plenum, New York, 1975), p. 323.
[14]P. Bergé and M. Dubois, in *Systems Far from Equilibrium, Proceedings of the Sitges International Conference,* 1980 (Springer, Berlin, 1981).
[15]A. C. Newell and J. A. Whitehead, J. Fluid Mech. 38, 279 (1969).
[16]L. A. Segel, J. Fluid Mech. 38, 203 (1969).
[17]R. Graham, Phys. Rev. A 10, 1762 (1974).

[18]J. Swift and P. C. Hohenberg, Phys. Rev. A 15, 319 (1977).
[19]S. N. Brown and K. Stewartson, Stud. Appl. Math. 57, 187 (1977).
[20]M. C. Cross, Phys. Fluids 23, 1727 (1980); see also R. E. Kelley and D. Pal, J. Fluid Mech. 86, 433 (1978).
[21]E. Siggia and A. Zippelius, Phys. Rev. Lett. 47, 835 (1981).
[22]J. Wesfried, Y. Pomeau, M. Dubois, C. Normand, and P. Berge, J. Phys. (Paris) Lett. 39 725 (1978).
[23]G. Ahlers, M. C. Cross, P. C. Hohenberg, and S. Safran, J. Fluid Mech. (in press).
[24]M. C. Cross (unpublished).
[25]Y. Pomeau and S. Zaleski, as in Ref. 8.
[26]J. Toner and D. R. Nelson, Phys. Rev. B 23, 316 (1981).
[27]The possible importance of grain boundaries was suggested to me by A. Zippelius (private communication).
[28]A. Schuter, D. Lortz, and F. Busse, J. Fluid Mech. 23, 129 (1965).
[29]M. M. Chen and J. A. Whitehead, J. Fluid Mech. 31, 1 (1968).
[30]K. Stork and U. Muller, J. Fluid Mech. 71, 231 (1975).
[31]P. Manneville, Phys. Lett. (in press).